

M.T. Preece
A.G. Osborn
S.S. Chin
J.G. Smirniotopoulos

Intracranial Neurenteric Cysts: Imaging and Pathology Spectrum

BACKGROUND AND PURPOSE: Intracranial neurenteric (NE) cysts are rare congenital lesions that may be mistaken for other, more common non-neoplastic cysts as well as cystic neoplasms. We delineate the imaging spectrum, pathologic findings, and differential diagnosis of NE cysts.

METHODS: History, imaging, surgical and pathologic findings were analyzed retrospectively in 18 patients with intracranial NE cysts. Fifteen were surgically proved cases; 3 exhibited classic imaging findings and are being followed clinically.

RESULTS: Thirteen cysts were located in the posterior fossa; 12 of 13 were extra-axial. Size varied from $1.2 \times 0.8 \times 0.6$ cm to $3.4 \times 3 \times 2.5$ cm. Five were supratentorial, measuring from $7 \times 5 \times 3$ to $9 \times 6 \times 7$ cm. All were frontal and off the midline. Seven of 18 patients had CT scans. Cysts varied widely in attenuation. None enhanced. Eighteen of 18 had MR images. Sixteen of 18 were hyperintense, and 2 were isointense to CSF on T1-weighted imaging. Sixteen of 18 were hyperintense on T2-weighted imaging. All cysts were hyperintense to CSF on fluid-attenuated inversion recovery (FLAIR) sequences. Diffusion imaging was performed on 2 patients. One case showed mild restriction. Mild posterior rim enhancement was seen in 5 cases at the site where the cyst adhered to brain parenchyma.

CONCLUSION: The imaging spectrum for NE cysts is broader than previously reported. Intracranial NE cysts should be considered in the differential diagnosis for intracranial extra axial cystic lesions both above and below the tentorium.

Neurenteric (NE) cysts, also called enterogenous cysts, are rare benign endodermal lesions of the central nervous system (CNS). They are approximately 3 times more common in the spine compared with the brain.¹ To date, fewer than 60 intracranial NE cysts have been reported in the literature.¹⁻³ Most are found in the posterior fossa, though rare supratentorial cysts have been reported.^{1,2,4,5} We delineate the imaging spectrum of 15 pathologically proved and 3 suspected intracranial cysts. We briefly discuss basic embryogenesis, pathology, and differential diagnosis of these cysts.

Methods

Case Selection

Eighteen unpublished cases collected from the University of Utah Medical Center, Primary Children's Medical Center, the Armed Forces Institute of Pathology, and the Columbia-Presbyterian Medical Center, NY, from 1990 to 2005, were reviewed retrospectively. Medical records, imaging studies, and surgical pathology were evaluated. In 15 cases, the diagnosis was based upon description of surgical findings and either review of histologic slides (6 cases) or pathology reports (9 cases). Pathologic material was not available in 3 cases that are being followed clinically. Imaging characteristics in these 3 non-surgical cases were reviewed by the senior author and were considered to be classic for NE cyst. These are regarded as sufficiently characteristic for definitive diagnosis and are included in Table 1 as "presumed NE cysts." Patients ranged in age from 12 to 78 years (average, 45.1 years). Thirteen patients were female and 4 were male. Patient information for one presumed cyst is unknown (Table 1).

Received September 28, 2005; accepted after revision January 23, 2006.

From the Departments of Radiology (M.T.P., A.G.O.) and Pathology (S.C.C.), University of Utah, Salt Lake City, Utah; and Department of Radiology and Nuclear Medicine (J.G.S.), Uniformed Services University, Bethesda, Md.

Address correspondence to Michael T. Preece, MD, 129 Franklin St, Apt 140, Cambridge, MA 02139.

Imaging

Seven of 8 patients were evaluated with CT. Both bone and soft tissue windows were evaluated in all 7 patients. All patients were evaluated with MR imaging performed at 1.5T. Contrast-enhanced scans were available in 14 of 18 cases. Fluid-attenuated inversion recovery (FLAIR) sequences were performed in 7 patients. Diffusion imaging was performed in 2 recent patients. The other studies were performed before the availability of diffusion-weighted MR imaging (DWI).

Results

Clinical Presentation

Patient history was available in 17 of 18 cases (Table 1). Headache was the major presenting complaint, reported in 8 of 17 patients (47.1%). Headaches varied from chronic tension-type to chronic migraine. Four of 17 patients had cranial nerve deficits (23.5%), including decreased gag reflex, decreased sensation in the distribution of V1 and V2, tinnitus, vertigo, and sensorineural hearing loss. Four of 17 had motor and sensory deficits, including numbness, paresthesias, incontinence, and gait disturbances (23.5%). Three of 17 presented with new onset seizure (17.6%). Two presented with recurrent meningitis (11.8%); 1 of these was the only patient in our series whose cyst was associated with a midline defect (Fig 1). One patient had a 5-month history of behavioral changes evolving into severe, acute psychosis.

Location and Size

Thirteen of 18 cysts were located within the posterior fossa (72.2%); 5 were supratentorial (27.8%). Seventeen cysts were extra-axial; 1 was located within the fourth ventricle. The most common location of the posterior fossa cysts was the lower cerebellopontine angle (8/13; 61.5%) and the midline pontomedullary junction (3 of 13; 23.1%). One was anterior to the lower medulla; 1 was in the fourth ventricle. Nine of 13 were

Table 1: Neuroradiologic findings

Patient No./ Age (y)/Sex	Location	Size (cm)	Symptoms	Bony Anomalies	NECT (Compared to Brain)	T1WI (Compared to CSF)	T2WI (Compared to Brain)	FLAIR (Compared to CSF)	T1 C+ (Enhancement)	DWI (Restriction)
1/46/F	Right lower CPA	1.2 × 0.8 × 0.6	Decreased gag reflex on right, decreased sensation in right V1 and V3 nerves	—	Isodense	Hyperintense	Hyperintense	Hyperintense	None	None
2/26/F	Midline, right lower CPA	2.6 × 1.6	Right-sided paresthesias; chronic migraine headaches	—	—	Hyperintense	Hyperintense	Hyperintense	None	—
3/39/F*	Midline, pontomedullary junction	0.6 × 1.4 × 1.1	Chronic headaches	—	—	Hyperintense	Hyperintense	Hyperintense	None	Mild
4/72/F	Left frontal lobe	8.8 × 4.6 × 6.6	Behavior changes leading to psychosis	—	Hypodense	Hyperintense	Hyperintense	Hyperintense	None	—
5/60/F	Midline, pontomedullary junction	1.5 × 0.8	Chronic headaches	—	—	Hyperintense	Hyperintense	—	—	—
6/unknown*	Lateral pontomedullary junction	1.5 × 1	—	—	—	Hyperintense	Hyperintense	Hyperintense	Posterior rim (at brain)	—
7/41/F	Midline, lower CPA	2.5 × 1.5	Chronic headache, tingling in distal extremities	—	—	Hyperintense	Hyperintense	—	Posterior rim (at brain)	—
8/57/F	Midline, 4th ventricle	3.4 × 3 × 2.5	Occasional vertigo, chronic occipital headache	—	—	Hyperintense	Hyperintense	—	None	—
9/12/F	Midline, lower CPA	1.4 × 1.8 × 0.8	History of recurrent meningitis	Midline cleft, CVJ	—	Hyperintense	Hyperintense	Hyperintense	—	—
10/70/M	Midline to right lower CPA	3 × 4	Incontinence, inability to walk	—	—	Hyperintense	Hyperintense	—	—	—
11/26/F	Midline, anterior to medulla	1.5 × 2	2 episodes "viral syndrome" (headache, fever, nausea, vomiting, nuchal rigidity, fever)	—	—	Hyperintense	Hyperintense	—	Posterior rim (at brain)	—
12/34/M	Left of midline, adjacent to calvarium, extending through left ethmoid	9 × 6 × 7	New onset seizures	—	Hypodense	Isointense	Hyperintense	—	None	—
13/21/F	Midline, anterior to brain stem extending into both CPA cisterns	3 × 2.5	"Migraines," persistent occipital headaches	—	Hyperdense	Hyperintense	Hypointense	Hyperintense	—	—
14/44/F	Lower left CPA	3 × 3	Progressive clumsiness of hands with gait disturbance	—	—	Hyperintense	Hyperintense	—	None	—
15/14/F	Right CPA	2 × 2 × 2	Long history of right-sided sensorineural hearing loss	—	—	Hyperintense	Hyperintense	—	Posterior rim (at brain)	—
16/78/F	Extra-axial right frontal lobe, with fluid-fluid levels	7 × 5 × 3	Acute onset single seizure	—	Isodense	iso-hyperintense	Hyperintense	—	None	—
17/48/M	Left intra/paraventricular, bilobed	8 × 5	2 weeks of tremor, numbness of right arm, and facial droop	—	Hyperdense, marginal Ca++ Hypodense	Hyperintense	Hyperintense	—	Thin marginal enhancement	—
18/78/M	Extra-axial, frontal lobe, multiple fluid-fluid levels	7 × 5 × 3	New onset seizure	—	Hyperdense	Hyperintense	Hyperintense	—	None	—

Note:—CPA indicates cerebellopontine angle; NECT, nonenhanced CT; T1WI, T1-weighted image; T2WI, T2-weighted image; T1 C+, T1 with gadolinium; DWI, diffusion-weighted image; CVJ, craniovertebral junction.
*Presumed neurenteric cyst

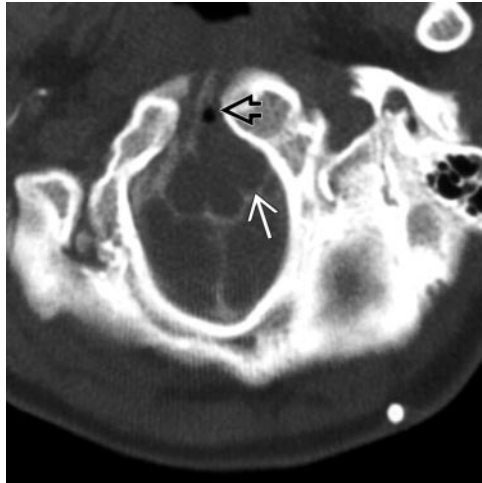


Fig 1. Patient 9. CT myelogram shows a well-delineated ovoid extra-axial mass (white arrow), at the foramen magnum level, associated with midline clefing of a craniocervical junction fusion anomaly (black open arrow). Bony anomalies are associated with approximately 50% of spinal NE cysts but have rarely been described in intracranial cases.

in, or extended into the midline (69.2%). The extra-axial posterior fossa cysts were consistently small, ranging in size from approximately 1×0.5 to 3×3 cm. The 5 supratentorial cysts were all significantly larger, measuring $7 \times 5 \times 3$ to $9 \times 6 \times 7$ cm. All were off-midline and located adjacent to the frontal lobes.

Imaging Findings

The imaging findings for each patient are summarized in Table 1. All 7 patients with nonenhanced CT (NECT) scans demonstrated a sharply demarcated cystic lesion. Three of 5 supratentorial cysts were hypoattenuated, 2 were isoattenuated, and 2 were hyperattenuated compared with brain. One patient had a contrast-enhanced CT scan and demonstrated no visible enhancement. Bony remodeling of the calvaria adjacent to the cyst was seen in 1 patient. One patient demonstrated hyperattenuated marginal calcification. Only 1 cyst was associated with a bony defect, midline clefing of a craniocervical junction fusion anomaly (Fig 1).

On MR imaging, all cysts were sharply demarcated and were typically oblong with smooth or lobulated margins. Sixteen of 18 were hyperintense compared with CSF on T1-weighted (T1WI) scans (88.9%) (Fig 2). Two cysts were isointense with CSF (11.1%). Sixteen of 18 cysts were hyperintense on T2-weighted sequences (88.9%) (Fig 3B). Two cysts were hypointense (11.1%). FLAIR sequences were performed in 7 cases. All cysts were hyperintense to CSF on FLAIR (Fig 4B). Imaging of the 2 cysts that were isointense to CSF on T1WI was performed before availability of FLAIR. Fourteen of 18 patients had contrast-enhanced T1WI. Nine of 14 showed no enhancement. Mild posterior rim enhancement was seen in 5 patients (35.7%) at the interface between the cyst and the adjacent brain parenchyma (Fig 5). Mild restriction was seen in 1 of the 2 available patients with DWI.

Pathology

Pathologic findings are summarized in Table 2. Microscopic examination of the excised cysts (Fig 6) revealed 2 major histologic patterns. The most common pattern was a cyst wall

that was notably poor in mucin-producing cells, seen in 7 of 15 patients. These cells were composed of pseudostratified, highly ciliated columnar epithelium (Fig 2C). Within these specimens areas of cuboidal epithelia were present, most evident in the largest supratentorial cyst (patient 4). The epithelial cells in this patient also exhibited prominent lipochrome-type pigment within the cytoplasm.

The second histologic pattern, seen in 4 patients, consisted of cyst epithelium that was rich in mucin-producing cells (Fig 7). Here, the cyst wall was composed of a simple columnar epithelium with nonciliated cells. Of the remaining 4 cases, all of which had only brief pathology report descriptions for review, 3 had no mention of mucin-producing cells, and 1 appeared to have a mixed histologic pattern with simple columnar and ciliated epithelium and was rich in mucin-producing cells. Two patients exhibited marked squamous metaplasia of the epithelium and voluminous keratinous material within the cyst space. The subepithelial tissue was uniformly composed of thickened layers of collagenous connective tissue. In 3 of the cases, foci of chronic inflammatory cell infiltrates were present. No cyst had evidence of either gross or microscopic hemorrhage. Analysis of cyst fluid composition was not performed.

Imaging-Pathology Correlation

The 13 of 18 patients for whom detailed histology was available were divided into 2 groups according to cyst cell wall pathology: "mucin-producing cell poor" (7 cases) or "mucin-producing cell rich" (6 cases). We analyzed CT attenuation and signal intensity in each case. Cysts were hyperintense on both T1WI and T2-weighted images (T2WI) in 5 of the 7 "mucin-producing cell poor" cases. Two patients in this group demonstrated hyperintense T1 signal intensity and hypointense T2 signal intensity. Three patients had NECT performed. Two cysts were isoattenuated; 1 was hyperattenuated.

Of the 6 cysts characterized as "mucin-producing cell rich," 5 were hyperintense on T1WI and T2WI; 1 was isointense on T1WI and hyperintense on T2WI. Only one mucin-producing cell rich cyst had available NECT and demonstrated hypoattenuation.

All but 2 of our patients had cyst contents that appeared hyperintense on T2WI. Both patients with hypointense T2 signal intensity exhibited marked squamous metaplasia of the epithelium and voluminous keratinous material within the cyst space.

Of the 5 lesions showing partial rim enhancement, only 1 was associated with chronic inflammatory changes. Pathologic data were not available for one patient, and the other 3 did not exhibit unique characteristics useful for correlation.

Discussion

Etiology and Pathogenesis

Neurenteric cysts, along with Rathke cleft and colloid cysts, are endodermally derived lesions of the CNS. First described by Puusep in 1934, NE cysts have had several names, including enterogenous cyst, enteric cyst, endodermal cyst, gastroenterogenous cyst, gastrocytoma, intestinoma, and archenteric cyst.^{1,6-9} Most reported NE cysts occur in the spine, usually ventral to the spinal cord.^{6,10-12} Spinal NE cysts are associated with vertebral anomalies in 50% of cases.^{1,12}

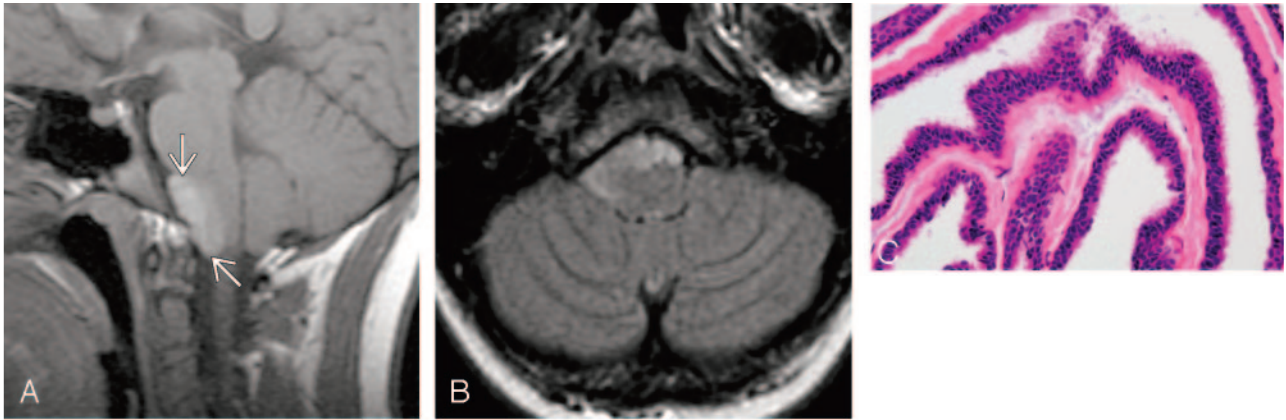


Fig 2. Patient 2.

A, Sagittal T1-weighted image demonstrates an ovoid mass (arrows) in the midline anterior to the pontomedullary junction. The cyst is hyperintense to brain parenchyma and CSF (reproduced from Osborn AG, et al, *Diagnostic Imaging: Brain*, Amirsys/Elsevier, 2004).

B, Axial FLAIR scan in the same patient shows that the mass remains hyperintense and extends from the midline into the right lower cerebellopontine angle.

C, Representative histopathology of a NE cyst showing pseudostratified, ciliated, columnar epithelium, which is poor in mucin-producing cells.

In contrast, intracranial NE cysts are uncommon, with less than 60 cases reported before our series.^{1,3,13} Intracranial cysts are most often found in the posterior fossa. They are typically midline, anterior to the brain stem, or in the cerebellopontine angle.⁴ They have also been described in the fourth ventricle.¹⁴ They occur in all age groups.³ With rare exception (Fig 1), intracranial NE cysts have not been associated with bony anomalies.^{3,8} Supratentorial NE cysts are rare, with only 14 cases reported.²

A review of prior cases demonstrates a slight male predominance among patients with intracranial NE cysts (60%).³ In this series, however, there is a clear female predominance; they represent 76.5% of the patients (13/17). It would thus seem that actual prevalence of neurenteric cysts is likely to be independent of sex.

The precise etiology of the NE cyst is unknown.^{6,15} One generally accepted theory suggests that they arise at the time of notochordal development during the transitory existence of the NE canal. The notochord and foregut fail to separate during the process of excretion, causing primitive endodermal cells to be incorporated into the notochord. These displaced nests of alimentary tissue ultimately become the cyst.^{6,7,16-18} This theory fails to explain the supratentorial cyst, however, because the cranial aspect of the notochord forms the posterior clinoid portion of the clivus.^{2,6} Any lesion cranial to the clivus would not take part in notochordal development. The Seessel pouch, an endodermal diverticulum found behind the oropharyngeal membrane, has been proposed as a possible embryologic progenitor of midline supratentorial cysts.^{2,3} This theory still fails, however, to explain off-midline supratentorial cysts.

Imaging

The signal intensity characteristics of intracranial cysts vary depending upon protein content of the cyst fluid.^{16,19-22} Most are proteinaceous with a T1 signal intensity that is isointense to slightly hyperintense compared with CSF and typically very hyperintense on T2WI, unless inspissated. The classic NE cyst as described in the literature is an ovoid/lobulated, nonenhancing, slightly hyperintense mass in front of the medulla. Most are small, measuring less than 2 cm. NE cysts are hyperintense on FLAIR and may show mild restriction on diffusion-weighted images.

Rim enhancement on reported cases is rare.^{1,20-22} Calcification has been described in only one supratentorial cyst.⁴

In our series, we found the imaging spectrum to be broader than previously described. As expected, all cases demonstrated isointense to hyperintense T1 signal intensity compared with CSF. Also as expected, T2WI showed some variability; 88.9% were hyperintense, and 11.1% were hypointense to CSF. Six of 18 cysts did not fit the paradigm of a typical posterior fossa location in the cerebellopontine angle or anterior to the brain stem. One posterior fossa cyst was an expansile lesion located within the fourth ventricle. Five cysts were large extra-axial masses adjacent to the frontal lobe. A clear differentiating feature between the supratentorial and posterior fossa lesions is size. All supratentorial cysts were larger than their posterior fossa counterparts. Two additional unexpected findings of our series included partial rim enhancement with a surprising prevalence of 35.7% and marginal calcification in a single supratentorial cyst.

In patient 11, partial rim enhancement was consistent with reactive changes occurring where the cyst attached to brain parenchyma. The microscopic interface between cyst and brain stem showed abundant mucus, surrounding chronic inflammation, foreign body reaction, and granulation tissue. These findings confirmed the surgical impression of previous cyst rupture. However, the other 3 cysts with partial rim enhancement and available histology showed no evidence of chronic inflammatory changes. In addition, patients 4 and 8 exhibited chronic inflammation without appreciable rim enhancement. Therefore, no definitive correlation can be made between chronic inflammatory changes and rim enhancement.

Pathology

NE cysts have been described to have variable appearances on light microscopy, as reflected by the many names that have been used to describe them. In our series, we note 2 major histologic patterns—one composed of pseudostratified, ciliated, columnar to cuboidal, mucin-producing cell poor epithelium and the other of simple, nonciliated, mucin-producing cell rich epithelium.

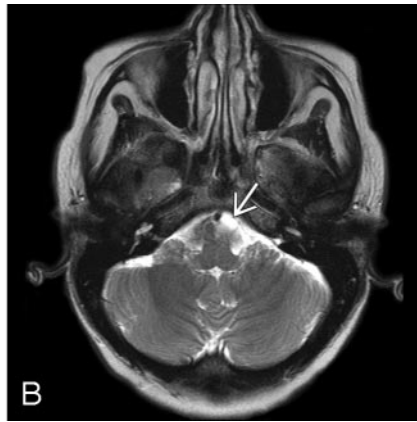


Fig 3. Patient 3.

A, Axial T1-weighted demonstrates an ovoid mass (arrow) slightly to the left of midline at the level of the pontomedullary junction. It is hyperintense to CSF and isointense to the surrounding brain parenchyma.

B, Axial T2-weighted image in the same patient demonstrates that the cyst is isointense to slightly hyperintense compared with CSF (arrow). Imaging findings are typical for NE cyst.

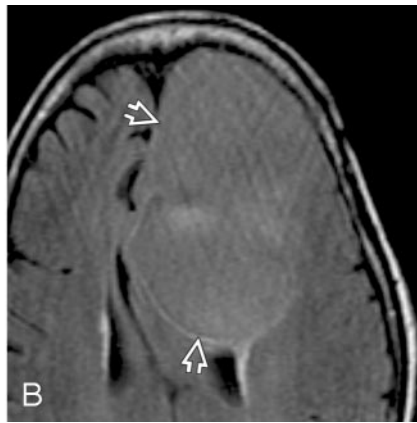
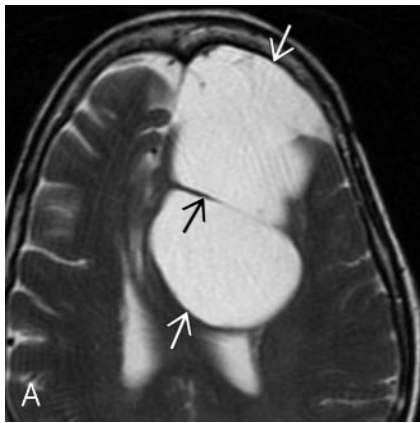


Fig 4. Patient 4.

A, Axial T2-weighted scan shows a huge extra-axial cyst (white arrows) with septation (black arrow) that displaces the corpus callosum posteriorly.

B, Axial FLAIR image in the same patient shows that the cyst fluid (open arrows) does not suppress and remains hyperintense compared with CSF. NE cyst was found at surgery. This lesion is unusual because of its supratentorial location and size. The rim of hyperintensity posteromedial to the cyst probably represents compressed brain, not the cyst wall itself, which is a single cell layer. The hyperintensity in the center of the lesion was not seen on any other images and is probably an artifact.

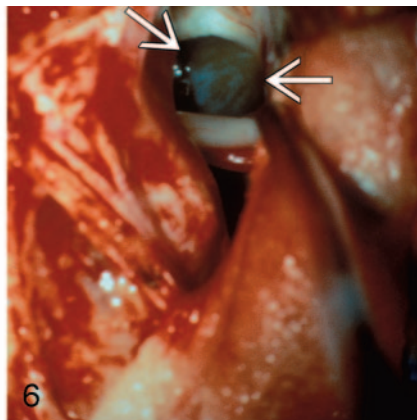


Fig 5. Patient 7. Sagittal postcontrast T1-weighted scan showing a large, well-delineated extra-axial mass (arrows) elevating and displacing the pons and medulla. The mass is slightly hyperintense compared with CSF. Slight rim enhancement is seen posteriorly, where the mass adheres to the brain parenchyma (open arrow). Cyst with watery, slightly cloudy fluid was found at surgery. Microscopic examination showed cyst lining composed of columnar epithelium with goblet cells, typical for NE cyst. Mild inflammatory changes in the cyst wall adjacent to the brain stem were present. Etiology of the rounded hyperintensity superior to the cyst is unexplained; the surgeons found nothing at the operation that clarified its nature. Postoperative changes of a prior occipital decompression for “Chiari 1” malformation are present (reproduced from Osborn AG, et al. *Diagnostic Imaging: Brain*, Amirsys/Elsevier, 2004).

Fig 6. Patient 13. Intraoperative photograph of a NE cyst in situ. The cyst is anterior to the brain stem with extension into both cerebellopontine angle cisterns. At surgery, this greenish cyst was found to be adherent to multiple structures.

These 2 histologic patterns correspond, respectively, to the respiratory and gastrointestinal features attributed to these lesions in the literature.^{6,8}

Although it would seem intuitive that a mucin-rich or -poor wall would affect cyst protein concentration, comparison of cyst wall histology with the imaging characteristics demonstrated no consistent correlation. In addition, differing cyst attenuation by NECT demonstrated no characteristic pathologic finding. No hemorrhage was seen by histology. An interesting pathologic correlate was found in the 2 cases that were T2 hypointense. The imaging finding is consistent with elevated protein concentration within the cyst.²² Results of pathologic examination in both patients demonstrated squamous metaplasia and voluminous keratinous debris.

Differential Diagnosis

The differential diagnosis for intracranial NE cyst includes epidermoid cyst, dermoid cyst, arachnoid cyst, and other endodermal cysts (Rathke and colloid).^{1,12,18,23,24} The rare “white” epidermoid is most similar to the NE cyst in that it is hyperintense on T1WI and can be difficult to distinguish if midline.¹⁹ Diffusion imaging can offer valuable information as epidermoid and dermoid lesions show moderate to striking diffusion restriction.¹¹ The diffusion may not offer definitive proof, however, given the enigmatic finding of partial diffusion restriction in 1 case of our series. Arachnoid cysts follow CSF on all sequences. Other endodermal-derived cysts, such as Rathke and colloid, can be differentiated from NE cysts based on location.¹⁴ Neoplasms including nerve sheath tumors can

Table 2: Neuropathologic findings

Patient No./ Age (y)/Sex	Pathology
1/46/F	Pseudostratified ciliated, columnar to cuboidal; mucin-producing cell poor
2/26/F	Pseudostratified, ciliated, columnar to cuboidal; mucin-producing cell poor—squamous metaplasia; voluminous keratinous material
3/39/F*	—
4/72/F	Low pseudostratified, ciliated, columnar to cuboidal; mucin-producing cell poor; lipochrome rich; focal chronic inflammation in stroma
5/unknown	Pseudostratified ciliated, columnar to cuboidal; mucin-producing cell poor
6/unknown*	—
7/41/F	Simple columnar; mucin-producing cell rich; mineralization in cyst space
8/58/F	Simple columnar; mucin-producing cell rich; focal chronic inflammation in stroma; focal mineralization in stroma
9/12/F*	—
10/70/M	Simple columnar, ciliated; mucin-producing cell rich
11/26/F	Simple columnar; chronic inflammation in stroma
12/34/M	Simple columnar to cuboidal; mucin-producing cell rich
13/21/F	Pseudostratified, ciliated, columnar; mucin-producing cell poor; squamous metaplasia—voluminous keratinous material
14/44/F	Simple cuboidal; mucin-producing cell rich
15/14/F	Simple cuboidal; mucin-producing cell rich
16/78/F	Pseudostratified ciliated columnar; mucin-producing cell poor
17/48/M	“Stratified” columnar (probably pseudostratified, ciliated); mucin-producing cell poor
18/78/M	Ciliated columnar

*Presumed neurenteric cyst.

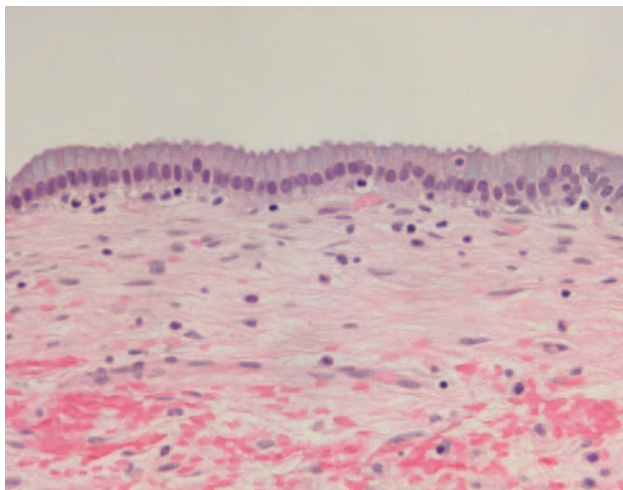


Fig 7. Patient 8. Representative histopathology of a NE cyst showing simple columnar to cuboidal epithelium that is rich in mucin-producing cells.

generally also be excluded from the differential diagnosis. These tumors (such as schwannoma) enhance strongly, are rarely in the midline, and are typically found associated with cranial nerves.

Conclusion

The imaging spectrum for neurenteric cysts is broader than previously described. Intracranial NE cyst should be considered in the differential diagnosis for any well-demarcated, extra-axial cystic lesion above or below the tentorium. Posterior fossa cysts tend to be small, nonenhancing lesions that are iso-intense to hyperintense on T1WI images, with variable T2 signal intensity. Partial rim enhancement may or may not be present. Supratentorial NE cysts are often much larger than posterior fossa cysts. They too are typically extra-axial and appear cystlike on MR images with smooth borders and no enhancement. These cysts should not be mistaken for more ominous pathologic entities such as neoplasms or infectious cysts.

References

- Osborn E, Blaser S, Salzman K, et al. Neurenteric cyst. *Diagnostic Imaging: Brain*. Amirsys 2004;1-7:40-41
- Christov C, Chretien F, Brugieres P, et al. Giant supratentorial enterogenous cyst: report of a case, literature review, and discussion of pathogenesis. *Neurosurgery* 2004;54:759-63
- Bejani GK, Wright DC, Schessel D, et al. Endodermal cysts of the posterior fossa: report of three cases and review of the literature. *J Neurosurg* 1998;89:326-35
- Tan GS, Hortobagyi T, Al-Sarraj S, et al. Intracranial laterally based supratentorial neurenteric cyst: case report. *Br J Radiol* 2004;77:963-65
- Cheng JS, Cusick JF, Ho KC, et al. Lateral supratentorial endodermal cyst: case report and review of literature. *Neurosurgery* 2002;51:493-99
- Harris C, Dias M, Brockmeyer D, et al. Neurenteric cysts of the posterior fossa: recognition management, and embryogenesis. *Neurosurgery* 1991;29:893-97
- Brooks B, Duvall E, El Gammal T, et al. Neuroimaging features of neurenteric cysts: analysis of nine cases and review of the literature. *AJNR Am J Neuroradiol* 1993;14:735-46
- Eynon-Lewis N, Kitchen N, Scaravilli F, et al. Neurenteric cyst of the cerebellopontine angle: case report. *Neurosurgery* 1998;42:655-58
- Kim CY, Wang KC, Choe G, et al. Neurenteric cyst: its various presentations. *Childs Nerv Syst* 1999;15:333-41
- Muthukumar N, Arunthathi J, Sundar V. Split cord malformation and neurenteric cyst—case report and a theory of embryogenesis. *Br J Neurosurg* 2000;488-92
- Inoue T, Kawahara N, Shibahara J, et al. Extradural neurenteric cyst of the cerebellopontine angle: case report. *J Neurosurg* 2004;100:1091-93
- Gao P, Osborn AG, Smirniotopoulos JG, et al. Neurenteric cysts: pathology, imaging spectrum, and differential diagnosis. *Int J Neuroradiol* 1995;1:17-19
- Bavetta S, El-Shunnar K, Hamlyn PJ. Neurenteric cyst of the anterior cranial fossa. *Br J Neurosurg* 1996;10:225-27
- Afshar F, Sholtz CL. Enterogenous cyst of the fourth ventricle: case report. *J Neurosurg* 1981;54:836-38
- Rauzzino MJ, Tubbs RS, Alexander E, et al. Spinal neurenteric cysts and their relation to more common aspects of occult spinal dysraphism. *Neurosurg Focus* 2001;10:Article 2
- Kapoor V, Johnson DR, Fukui MB, et al. Neuroimaging-pathologic correlation in a neurenteric cyst of the clivus. *AJNR Am J Neuroradiol* 2002;23:476-79
- Pang D, Dias MS, Ahab-Barmada M. Split cord malformation: part I: a unified theory of embryogenesis for double spinal cord malformations. *Neurosurgery* 1992;31:451-80
- Lonjon M, Paquis P, Michiels JF, et al. Endodermal cyst of the foramen magnum: case report and review of the literature. *Childs Nerv Syst* 1998;14:100-03
- Ochi M, Hayashi K, Hayashi T, et al. Unusual CT and MR appearance of an epidermoid tumor of the cerebellopontine angle. *AJNR Am J Neuroradiol* 1998;19:1113-15
- Shakudo M, Inoue Y, Ohata K, et al. Neurenteric cyst with alteration of signal intensity on follow-up MR images. *AJNR Am J Neuroradiol* 2001;22:496-98
- Evans A, Stoodley N, Halpin S. Magnetic resonance imaging of intraspinal cystic lesions: a pictorial review. *Curr Probl Diagn Radiol* 2002;31:79-94
- Hayashi Y, Tachibana O, Muramatsu N, et al. Rathke cleft cyst: MR and biomedical analysis of cyst content. *J Comput Assist Tomogr* 1999;23:34-38
- Chaynes P, Thorn-Kany M, Sol JC, et al. Imaging in neurenteric cysts of the posterior cranial fossa. *Neuroradiology* 1998;40:374-76
- Simon JA, Olan WJ, Santi M. Intracranial neurenteric cysts: a differential diagnosis and review. *RadioGraphics* 1997;17:1587-93